Available online at www.sciencedirect.com

SciVerse ScienceDirect

Acta Materialia 59 (2011) 7082–7094

Acta MATERIALIA

www.elsevier.com/locate/actamat

Thermal annealing of shear bands in deformed metallic glasses: Recovery mechanisms in $Cu_{64}Zr_{36}$ studied by molecular dynamics simulations

Yvonne Ritter *, Karsten Albe

Institut für Materialwissenschaft, TU Darmstadt, Petersenstr. 32, D-64287 Darmstadt, Germany

Received 27 June 2011; received in revised form 26 July 2011; accepted 28 July 2011
Available online 24 August 2011

Abstract

Molecular dynamics simulations on the recovery of shear bands in deformed binary $Cu_{64}Zr_{36}$ glasses are presented. While the shear band (SB) formation induced by plastic deformation leads to an increase in excess volume, the material surrounding the SB experiences a compressive strain due to the dilatation of the SB. This is accompanied by changes in topological and chemical short-range order within the shear band. Isothermal annealing of the sample leads to redistribution and annihilation of excess volume, which is coupled to the recovery of local order and depends on the temperature. At lower temperatures (500 K) diffusion by a chain-like process is the dominating mechanism of structural recovery, similar to processes occurring in supercooled liquids. At higher temperatures (800 K) individual atomic displacements also start to contribute to the recovery process. At temperatures close to the glass transition, the recovery occurs on timescales of about 20 ns. If the annealing temperature is higher than T_g, thermal activation is sufficient to rejuvenate the glass structure.

Keywords: Metallic glasses; Shear bands; Recovery; Annealing; Molecular dynamics

1. Introduction

Plastic deformation of metallic glasses at low temperatures and high strain rates is usually highly localized, occurring in narrow shear bands [1]. These shear bands are two-dimensional planar defects, which are characterized by an increased free volume [2–4] and a more disordered structure [1,5] in terms of chemical (CSRO) as well as topological short-range order (TSRO). The highly deformed material inside a shear band acts like a second phase with lower density, lower elastic modulus and yield strength [6,7], and increased diffusivity [8]. Due to the limited atomic mobilities under ambient conditions, shear bands still contain the same amount of excess volume after the applied stress is removed [5] and remain weak points in a deformed metallic glass sample. When annealed at elevated temperatures (below the glass transition temperature T_g), however, shear bands recover substantially by annihilation of the excess volume and relaxation of the short-range order (SRO) [1,3,5,8–10], wherefore the strain softening due to plastic deformation is reversed [8]. After annealing, pre-deformed and recovery-annealed samples still exhibit an enhanced ductility as compared to the virgin material [9] and preferential etching is still observed for the relaxed shear bands [5]. One possible explanation for the incomplete recovery is that structural relaxation only requires diffusion distances of less than an atomic diameter, whereas the re-establishment of chemical order requires long-range diffusion, which is not achieved under the given annealing conditions [5]. This assumption, however, is contradictory to earlier reports stating that changes in the chemical short-range order require only minor changes of the local chemical surroundings, whereas changes in the TSRO require larger rearrangements [11,3].

In the framework of free volume theory, it appears rather surprising that shear bands do not recover instantaneously

* Corresponding author.
E-mail address: ritter@mm.tu-darmstadt.de (Y. Ritter).

1359-6454/$36.00
doi:10.1016/j.actamat.2011.07.063

when subjected to thermal annealing at high temperatures: an increase in free volume, as observed in shear bands, is related to an increase in fictive temperature and, consequently, a decrease in the viscosity of the glass [12]. At high temperature, the local atomic mobilities and relaxation times should therefore be equivalent to mobilities and relaxation times in the supercooled liquid, leading to fast recovery of structural defects. However, experimental observations contradict this, with the recovery of deformed samples at high temperature occurring on timescales in the range of hours. This inconsistency begs the need for a detailed investigation on thermal annealing of plastically deformed metallic glasses to elucidate the atomic scale mechanisms involved in structural relaxation.

In this work, we study the annealing behavior of a pre-deformed $Cu_{64}Zr_{36}$ glass at different temperatures below and above T_g by molecular dynamics (MD) simulations. First, the sample is deformed under uniaxial tension and the mechanisms involved in shear band formation are characterized in terms of free volume and SRO. Secondly, shear band recovery on the atomic scale during unloading and annealing is investigated and the atomic scale diffusional mechanisms driving the recovery are analyzed in detail.

2. Methods

To studying the recovery of shear bands in pre-deformed metallic glass during thermal annealing, we performed classical MD simulations [13] using the modified Finnis-Sinclair type potential for Cu–Zr by Mendelev et al. [14]. An amorphous $Cu_{64}Zr_{36}$ sample was prepared by cooling the melt: after relaxation at 2000 K for 2 ns to ensure chemical homogeneity, the melt was quenched to 50 K at a cooling rate of 0.01 K ps^{-1}. The atomic structure of the synthesized $Cu_{64}Zr_{36}$ glass exhibited good agreement with data reported in the literature (e.g. Ref. [15]).

We simulated uniaxial tensile deformation of a 3 dim.-periodic sample ($36 \times 8 \times 26\ nm^3$; 432,000 atoms) by applying a constant strain rate of $4 \times 10^7\ s^{-1}$ in the z-direction at a constant temperature of 50 K. The pressure in the x- and y-directions was kept at 0 kbar to allow for lateral contraction. At a strain of 14%, after one extended shear band had formed, the sample was unloaded to zero stress. The previously deformed and unloaded sample was then heated at a rate of 0.1 K ps^{-1}, annealed for 20 ns at 500 K ($\approx 0.55T_g$), 800 K ($\approx 0.85T_g$) and 1000 K ($\approx 1.05T_g$), and subsequently quenched to 50 K, again at a rate of 0.1 K ps^{-1}. For comparison, an as-prepared $Cu_{64}Zr_{36}$ glass sample ($8 \times 5 \times 12\ nm^3$; 32,000 atoms) was subjected to the same thermal treatments.

The short-range order and packing density were analyzed using the Voronoi tessellation method [16,17], which divides the simulation cell into Voronoi polyhedra (VPs) around each atom taking into account the different atomic radii in the binary metallic glass. A VP is defined as the minimal polyhedron whose planar faces bisect the

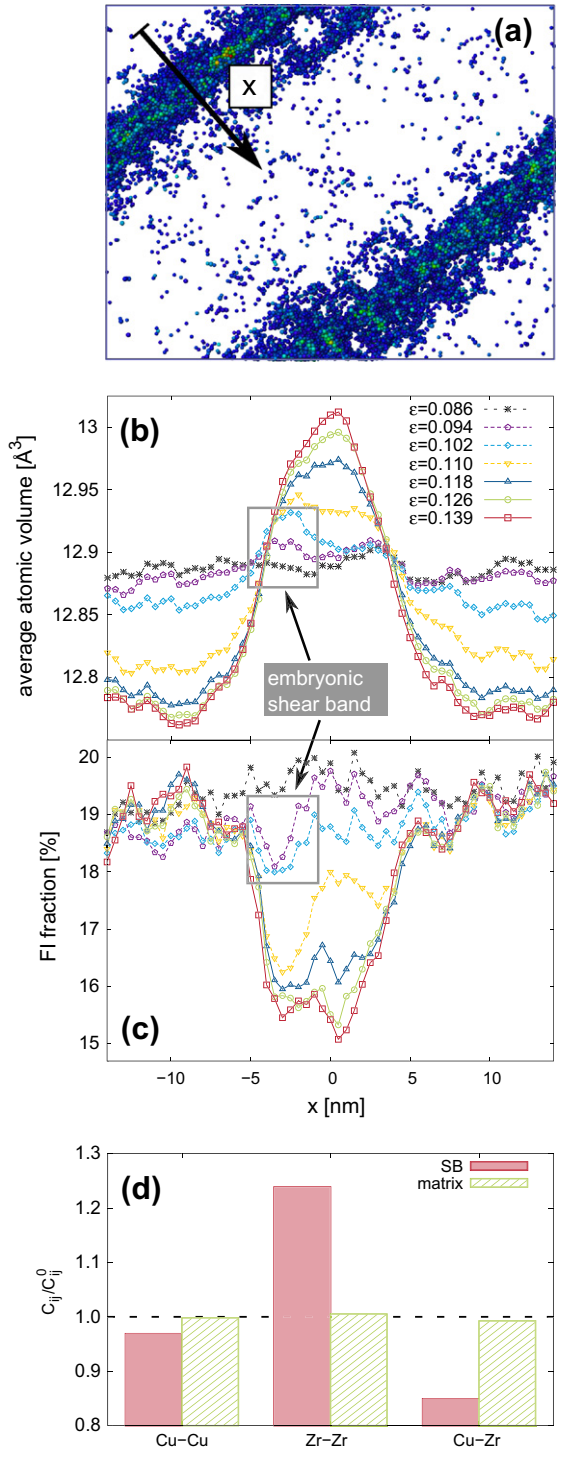

Fig. 1. Shear band characterization: (a) snapshot of deformed sample with SB; the atoms are colored according to their local atomic strain η_i^{Mises} (blue: $\eta_i^{Mises} = 0.2$, red: $\eta_i^{Mises} = 0.5$) [22]. For clarity, only atoms with $\eta_i^{Mises} > 0.2$ are displayed. (b) Linear scans of the average Voronoi volume of Cu atoms. (c) The fraction of Cu-centered full icosahedra at different strains during tensile deformation of a $Cu_{64}Zr_{36}$ glass. (d) Changes in the CSRO in the matrix and shear band after deformation. The nearest neighbor correlation indices are given with respect to the value for the undeformed sample C_{ij}^0. (For interpretation of the references to color in this figure legend, the reader is referred to the web version of this article.)

lines joining an atom to its neighboring atoms at right angles. The polyhedra can be characterized by the Voronoi index $[n_3,n_4,n_5,n_6]$, where n_i denotes the number of i-edged faces of the VP. In previous studies, the Cu-centered Voronoi polyhedron with index $[0,0,12,0]$ (=full icosahedron, FI) was found to be a key structural motif in amorphous Cu–Zr alloys, characterized by high packing density [18] and high shear resistance [15]. Inside shear bands, this structural backbone [19] is defective due to the high degree of plastic deformation. In the following, therefore, we have focused the characterization of topological short-range order on the population of Cu-centered full icosahedra.

In addition to the information on TSRO, the Voronoi analysis yields a Voronoi volume for each atom. According to the definition by Turnbull and Cohen [20], we specify the excess volume as being the difference between the specific volume (analogous to the Voronoi volume) and the molecular volume (here: atomic volume). Assuming a constant atomic volume, an increase in Voronoi volume can be directly translated into an increase in excess volume.

To study the chemical short-range order, we calculated the nearest neighbor correlation index C_{ij} ($i,j=$ Cu, Zr) [21], which compares the distribution of Cu and Zr atoms in the metallic glass to a statistical distribution,

$$C_{ij}=\frac{p_{ij}}{p_{ij}^0}-1 \tag{1}$$

where p_{ij} is the probability of an atom of type i and an atom of type j being neighbors in the analyzed structure, and p_{ij}^0 is the value for an uncorrelated distribution. This probability is calculated as $p_{ij}=m_{ij}/p_{total}$, where m_{ij} is the number of nearest neighbor (NN) pairs of type ij and p_{total} is the total number of nearest neighbor pairs. The uncorrelated value is obtained from

$$p_{ij}^0=\begin{cases}\frac{n_i(n_i-1)}{N(N-1)} & \text{for } i\neq j\\ \frac{2n_in_j}{N(N-1)} & \text{for } i=j\end{cases}, \tag{2}$$

where $n_{i/j}$ is the number of atoms of type i/j in the system and N is the total number of atoms. A negative value for C_{ij} indicates a negative correlation, which means that atoms of type i have on average fewer j neighbors than in the statistical case, and vice versa.

For a comparative study of structural recovery inside the shear band and in the matrix, we analyzed the average Voronoi volumes, the fraction of Cu-centered FIs and the CSRO for a test volume of 2 nm thickness in the center of the shear band, as well as for a test volume in the matrix. In addition, we scanned the average volumes and FI fraction perpendicular to the SB slip direction, to gain more insight in the local structural rearrangements during deformation and thermal treatment. Each scan shown in Figs. 1 and 6 is an average of three single scans at different snapshots within a time interval of 300 ps, in order to minimize statistical fluctuations.

3. Results and discussion

3.1. Shear band characterization

In order to study shear band recovery and the underlying atomic scale mechanisms, it is necessary to first characterize the shear band (see the snapshot in Fig. 1a) itself, along with the structural changes occurring inside the shear band and the matrix during deformation. We therefore scanned the average atomic volumes and the fraction of Cu-centered full icosahedra for snapshots at different strains during tensile deformation (see Fig. 1b and c). The development of Cu and Zr Voronoi volumes during deformation is almost identical, thus only the results for the Cu volumes are shown in this section. The atomic volumes in the whole sample increase linearly and homogeneously up to a strain of about 9%, while the FI occupation decreases slowly in the whole sample from 22% in the virgin sample to 19.5%. At 9.4% strain, the scan of the FI fraction shows a local decrease, which is accompanied by an increase in the average Voronoi volume (see the marked position in Fig. 1b and c). This indicates the formation of an embryonic shear band, which subsequently grows to a width of 10 nm. From our results, the link between the destruction of FIs as a topological feature with high packing density and the creation of excess volume is obvious (we find the average Voronoi volume of a Cu atom in the center of an FI is 0.4 Å^3 lower than the average volume of other Cu atoms). While the SB propagates, excess volume is generated, which is seen as an increase in the Voronoi volumes inside the SB. At the same time, the atomic volumes in the undeformed matrix decrease as a result of a compressive stress component introduced by the volume expansion of the shear band. The TSRO in the matrix is hardly affected since all deformation occurs localized inside the shear band, and the occupation of Cu-centered full icosahedra remains constant. In the unloaded sample, the Voronoi volumes in the SB are about 0.25 Å^3 (or 2.0%) higher than in the matrix and the FI fraction is 6% lower.

Since not only the topological but also the CSRO of metallic glasses is affected by deformation and annealing, we also compared the nearest neighbor correlation index C_{ij} ($i,j=$ Cu, Zr) of the virgin $Cu_{64}Zr_{36}$ glass and the deformed sample. For the undeformed sample we find a negative correlation for Cu–Cu neighbors ($C_{Cu,Cu}=-0.24$) and positive correlations for the Zr–Zr and Cu–Zr neighbors ($C_{Zr,Zr}=0.16$ and $C_{Cu,Zr}=0.17$). Given these deviations from a statistical alloy, we conclude that CSRO is present in the as-prepared $Cu_{64}Zr_{36}$ glass. Fig. 1d shows the effect of plastic deformation on the CSRO: upon deformation, the CSRO in the matrix remains almost unchanged ($\Delta C_{Cu,Cu}=+0.2\%$, $\Delta C_{Zr,Zr}=+0.5\%$, and $\Delta C_{Cu,Zr}=-0.7\%$), while the values for the highly strained material inside the shear band indicate significant changes in the CSRO. The degree of correlation for the Cu–Cu and Cu–Zr neighbors is decreased by 3% and 15%, respec-

tively, while the magnitude of the Zr–Zr correlation is increased by 24%.

In summary, we find the shear band to be characterized by an increased excess volume, a lower degree of TSRO and a modified CSRO. The short-range order in the matrix is hardly affected during deformation; only the atomic density is increased due to a compressive strain introduced by the shear band.

3.2. Structural relaxation of undeformed $Cu_{64}Zr_{36}$ glass

The main goal of this study was to gain a better understanding of the structural relaxation of plastically deformed metallic glasses. Yet, even an as-prepared metallic glass is thermodynamically unstable and thermally activated atomic rearrangements lead to an increase in the overall configurational order of the system, namely an increase in packing density and an increase in chemical and TSRO. Consequently, if we want to distinguish between the relaxation processes always occurring in a glass that was obtained by rapid quenching and the recovery of defects caused by plastic deformation, we first have to analyze an as-quenched (=virgin) metallic glass under annealing conditions.

Fig. 2 shows the evolution of the Voronoi volume of Cu and Zr atoms relative to the initial volume, the content of Cu-centered full icosahedra (middle panels) and the CSRO (bottom panels) during annealing at 500, 800 and 1000 K. Before comparing the results for the different annealing temperatures, we should point out two general features that are present in all three cases. (i) When comparing the relative Voronoi volumes of Cu and Zr atoms during heating, the larger thermal expansion for Cu atoms stands out. The volume coefficients of thermal expansion below T_g can be estimated by

$$\alpha_v = \frac{\Delta V}{V_0 \cdot \Delta T} = \frac{V(500\ \mathrm{K}) - V(50\ \mathrm{K})}{V(50\ \mathrm{K}) \cdot 450\ \mathrm{K}} \tag{3}$$

Using the sample volume at 50 and 500 K, we get a value of $\alpha_v = 2.1 \times 10^{-5}\ \mathrm{K}^{-1}$ for the whole sample. This value is in good agreement with experimental values of thermal expansions for other metallic glasses reported in the literature (e.g. Refs. [3,12]). The partial thermal expansion coefficients for Cu and Zr atoms are approximated by inserting the appropriate average Voronoi volumes into Eq. (3). Using this approach we get values of $\alpha_v^{Cu} = 2.5 \times 10^{-5}\ \mathrm{K}^{-1}$ and $\alpha_v^{Zr} = 1.9 \times 10^{-5}\ \mathrm{K}^{-1}$. One possible explanation for this difference in thermal expansion is stronger anharmonicity in the interatomic potential for Cu atoms as compared to Zr atoms. In order to confirm this assumption, we simulated energy volume curves for Cu and Zr (see Fig. 3). We therefore homogeneously strained the virgin glass sample to a fixed volume, let the atomic positions relax and determined the potential energy contribution of Cu atoms and Zr atoms. The resulting curves were fitted by the Birch–Murnaghan equation of state [23], and the pressure derivative of the isothermal bulk modulus B'_T, which is a measure for the anharmonicity of the potential, was evaluated. From B'_T, we can approximate the Grüneisen parameter $\gamma \approx \frac{1}{2}(B'_T - 1)$ [24], which is directly

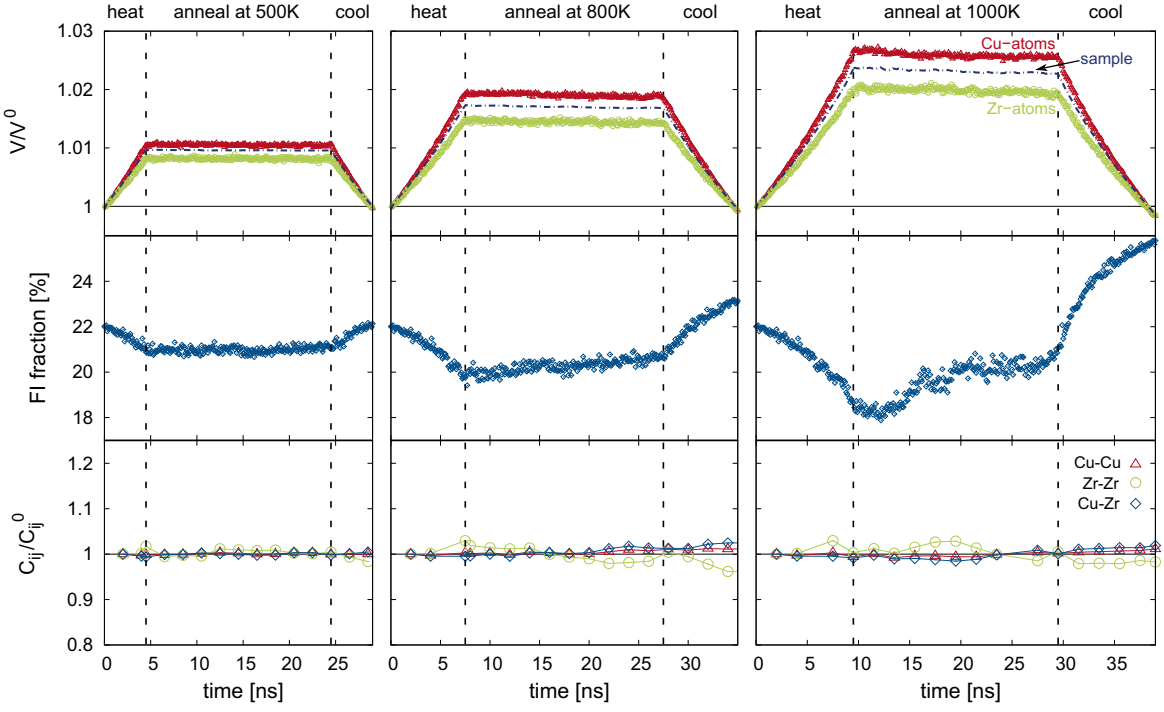

Fig. 2. Annealing of the as-quenched $Cu_{64}Zr_{36}$ glass: changes in relative volume, FI fraction and CSRO are shown for annealing temperatures of 500 K ($\approx 0.55T_g$), 800 K ($\approx 0.85\ T_g$) and 1000 K ($\approx 1.05T_g$). At 500 K, thermal activation is not sufficient to activate structural relaxations, while we observe a marginal release of excess volume and increase in FI fraction at 800 K. When the annealing temperature is above T_g, the glass structure relaxes substantially. The CSRO does not change significantly, independent of the temperature.

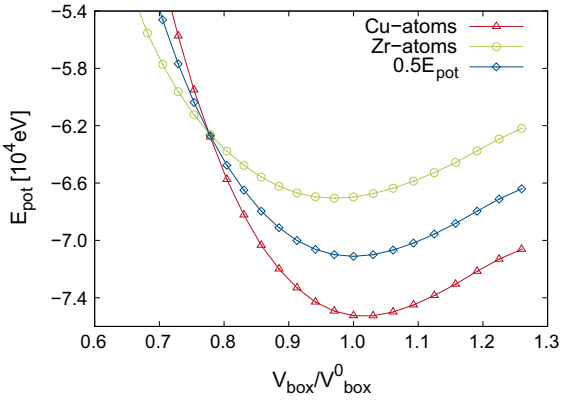

Fig. 3. Energy volume curves for Cu and Zr: a stronger anharmonicity in the interatomic potential for Cu atoms as compared to Zr atoms leads to a bigger thermal expansion for the Cu atomic volumes.

proportional to the thermal expansion; thus a larger γ means greater thermal expansion. Because of the strong variation of the fit results with the fitting interval, we calculated B'_T as a function of the fitting interval. Over the whole range of fitting intervals considered, we obtain a higher B'_T for Cu ($\approx$3.35) than for Zr ($\approx$2.9); the resulting Grüneisen parameters are $\gamma_{Cu} = 1.18$ and $\gamma_{Zr} = 0.95$. Consequently, the higher thermal expansion for Cu can be explained by the stronger anharmonicity of the interatomic potential for Cu atoms.

(ii) When the sample is heated, the population of Cu-centered full icosahedra decreases (see Fig. 2, middle panels). This decrease is a result of the anisotropic thermal expansion of the $Cu_{64}Zr_{36}$ metallic glass studied here, which leads to an elastic distortion of the icosahedral clusters in the sample and, therefore, the analysis detects a lower fraction of FIs. This effect is fully reversible and does not influence the results.

Next we compare the relaxation of excess volume, topological and chemical SRO in the undeformed sample at different temperatures. When the undeformed sample is heated to 500 K, the thermal expansion is linear, indicating that no excess volume is released during heating. During annealing at 500 K, changes in the Voronoi volumes (as well as the sample volume) are hardly detectable and the final volumes after quenching are almost identical to in the as-quenched case. So, on the timescales studied here, no excess volume is released at a temperature of 500 K. This is in good agreement with the behavior of the TSRO: taking statistical fluctuations into account, the FI fraction in the virgin sample is almost the same as the FI fraction after annealing at 500 K and subsequent quenching. The same holds true for the CSRO, where the changes during annealing are of the order of statistical fluctuations. During annealing at 800 K, we observe a marginal volume decrease and the final sample volume is 0.04% smaller than the virgin sample. Again, we find the excess volume to be linked to the FI fraction, which increases by approximately 1% during annealing at 800 K. As for an annealing temperature of 500 K, changes in the CSRO are of the order of statistical fluctuations and no significant trend is detected. The thermal expansion deviates from a linear behavior when the glass transition temperature is passed during heating to 1000 K. After annealing at $T > T_g$, a total amount of 0.14% free volume (with respect to the sample volume) is released and, at the same time, the FI occupation is increased by 4%. Interestingly, the volume release as well as the increase in the FI fraction only occur within the first 10 ns of annealing, before both saturate. A possible explanation for this is that, in the final structure, 78% of all atoms are incorporated in Cu-centered full icosahedra. Since dense packing is not possible using only FIs (due to its fivefold symmetry), packing frustration will occur at a certain FI density, when a further increase in the number of FIs would lead to a volume increase. Again, the CSRO does not change significantly.

To summarize this section, we have found that the thermal expansion for Cu atoms is larger than for Zr atoms. At an annealing temperature of 500 K, almost no structural relaxation occurred in the as-prepared $Cu_{64}Zr_{36}$ glass, while we observe an increase in the FI fraction accompanied by a decrease in excess volume at 800 and 1000 K. In agreement with our results on shear band formation above, changes in the TSRO are directly coupled to changes in the packing density. The CSRO is not changed by thermal annealing on the timescales studied here.

3.3. Shear band recovery

After analyzing the structural relaxation of an as-prepared bulk sample under annealing conditions, this section will focus on the structural recovery of a deformed metallic glass. Fig. 4 shows the evolution of the relative volumes of the sample and the Cu and Zr atoms (first and second rows of panels), changes in the FI fraction as an indicator for the TSRO (third and fourth rows of panels) and the relative nearest neighbor correlation indices representing variations in the CSRO (fifth row of panels), in shear band and matrix for annealing temperatures of 500 K, 800 K, and 1000 K. The relative volumes and correlation indices are given with respect to the corresponding values for the undeformed sample. Looking at the variation in the relative volumes (Fig. 4, top panels), it is obvious that the structural recovery of the deformed glass is overlayed with the thermal expansion. The same holds for the recovery of the icosahedral short-range order (Fig. 4, third row of panels), which is overlayed by the decreasing FI fraction due to anisotropic thermal expansion. Consequently, in order to analyze shear band relaxation, the data has to be deconvolved. In the case of the volume data, this is done by adapting the model of Taub and Spaepen [12], according to which the equilibrium thermal expansion of a glass α_{th} consists of an isoconfigurational contribution resulting from the anharmonicity of the interatomic potential α_{iso} and a structural change term reflecting the changes in packing density and chemical order during heating α_{struc}:

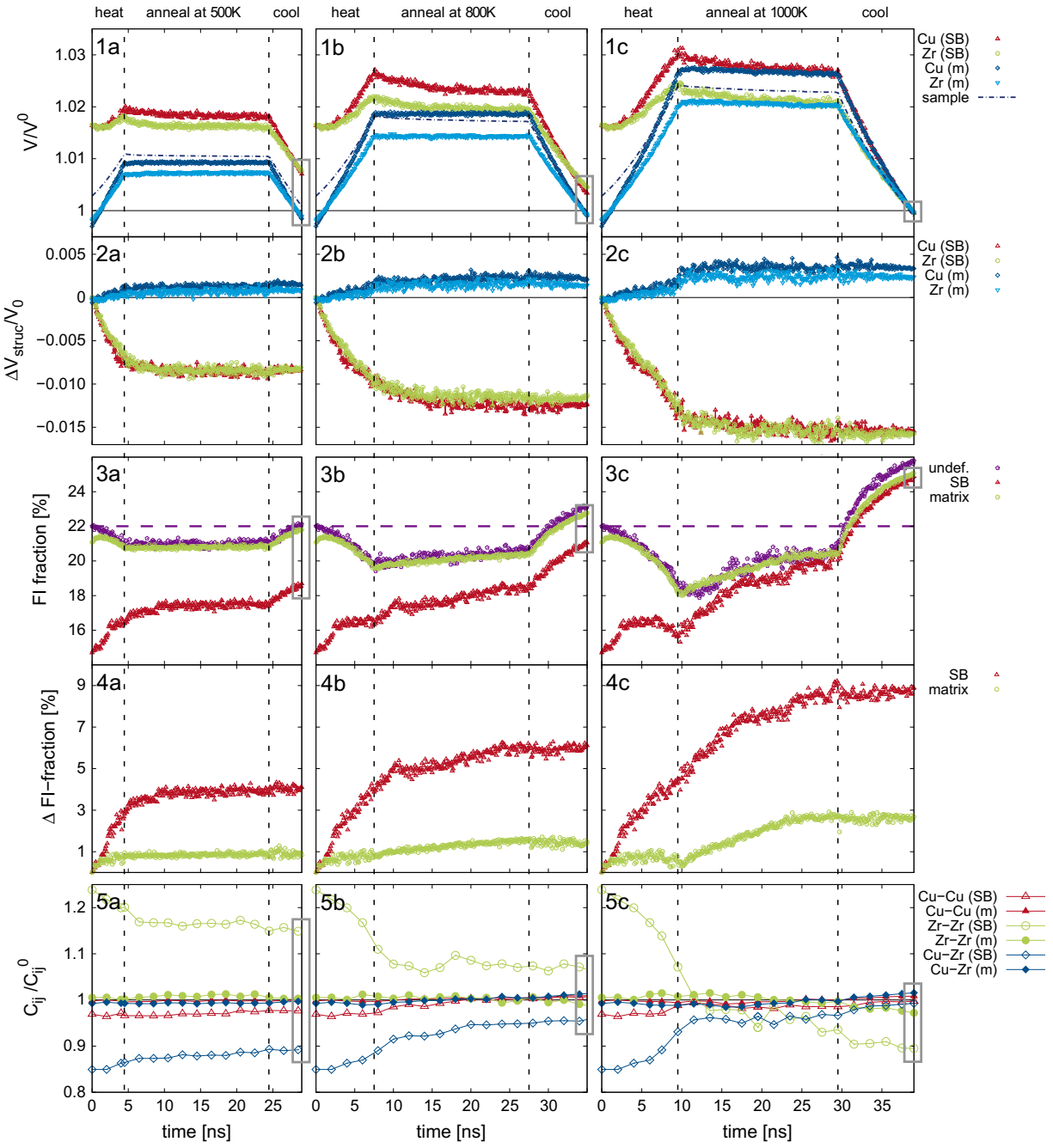

Fig. 4. Annealing of a pre-deformed sample: changes in relative volume (1a–c) and volume changes due to structural relaxation (2a–c), evolution of FI fraction (3a–c) and increase in FI fraction due to structural rearrangements (4a–c), and the recovery of the CSRO (5a–c) are shown for annealing temperatures of 500 K ($\approx 0.55T_g$), 800 K ($\approx 0.85T_g$) and 1000 K ($\approx 1.05T_g$). At 500 K, only the SB relaxes while the matrix remains unchanged; the thermal activation does not allow a full recovery. At 800 K, both the SB and the matrix undergo structural relaxation.

$$\alpha_{th} = \alpha_{iso} + \alpha_{struc} \tag{4}$$

Given the definition of the volume coefficient of thermal expansion in Eq. (3), we can write:

$$\frac{\Delta V_{def}}{V^0_{def}} = \frac{\Delta V^{iso}_{def}}{V^0_{def}} + \frac{\Delta V^{struc}_{def}}{V^0_{def}} \tag{5}$$

where ΔV_{def}, ΔV^{iso}_{def} and ΔV^{struc}_{def} are the total volume change, the volume change due to isoconfigurational thermal expansion and the volume change due to structural relaxation, and V^0_{def} is the volume of the deformed sample before heating or quenching, respectively. Since we do not know the isoconfigurational contribution to thermal expansion of the deformed sample, we approximate this quantity by the thermal expansion of the undeformed sample assuming that structural relaxations during heating of the virgin material are negligible on the timescales studied here. With this assumption, and with $\Delta V = V(T) - V_0$, we can

estimate the volume change resulting due to structural relaxation ΔV_{struc} by

$$\Delta V_{struc}(T) = V^0_{def}\left[\frac{V_{def}(T) - V^0_{def}}{V^0_{def}} - \frac{V_{undef}(T) - V^0_{undef}}{V^0_{undef}}\right] \quad (6)$$

In order to study the relaxation of the shear band and of the matrix separately, we calculated the average Voronoi volumes in a test volume inside the shear band and in the matrix, and compared them to the according average Voronoi volumes in the undeformed sample to evaluate Eq. (6). The resulting volumetric changes are identical to changes in excess volume due to the recovery of structural defects introduced by plastic deformation (see Fig. 4, second row of panels).

In order to eliminate the effect of anisotropic thermal expansion from the evolution of the FI occupation, we again compare data for the deformed sample to data for the undeformed sample, using the following relation:

$$\Delta c^{FI}_{struc}(T) = c^{FI}_{def}(T) - \Delta c^{FI}_{undef}(T) \quad (7)$$

where Δc^{FI}_{struc} is the change in FI fraction due to structural recovery, $c^{FI}_{def}(T)$ is the FI fraction in the deformed sample at temperature T and $\Delta c^{FI}_{undef}(T)$ is the corresponding change in FI fraction during heating/quenching of the undeformed sample. Using this approach, we obtain the absolute changes in FI fraction during heating, annealing and quenching (see Fig. 4, fourth row of panels).

The results shown in Fig. 4 illustrate that the recovery of a deformed metallic glass involves the relaxation of excess volume, TSRO and CSRO: independent of the annealing temperature, we observe a decrease in excess volume in the shear band, while the excess volume in the matrix increases (see the second row of panels). The reason for the volume increase in the matrix is that excess volume is transported from the SB into the surrounding material, which was subjected to a compressive strain during SB formation and therefore recovers by the absorption of excess volume. The fraction of Cu-centered FIs increases in the SB as well as in the matrix (see the fourth row of panels) and the CSRO, which was only affected inside the SB, tends to go back to the initial state before deformation (see the fifth row of panels). As mentioned in the previous sections, we find a strong connection between the local concentration of Cu-centered full icosahedral clusters and the packing density or excess volume, respectively. In order to further investigate the nature of this correlation, we plotted the change in Voronoi volume due to structural relaxation against the corresponding change in FI fraction in the shear band during heating, annealing and quenching for different annealing temperatures. The resulting graph (see Fig. 5) reflects the aforementioned observations: we see a linear decrease in the Voronoi volumes, which is equivalent to a decrease in excess volume with increasing FI fraction, at least if the temperature is below T_g. For temperatures above T_g, the data points deviate from the linear

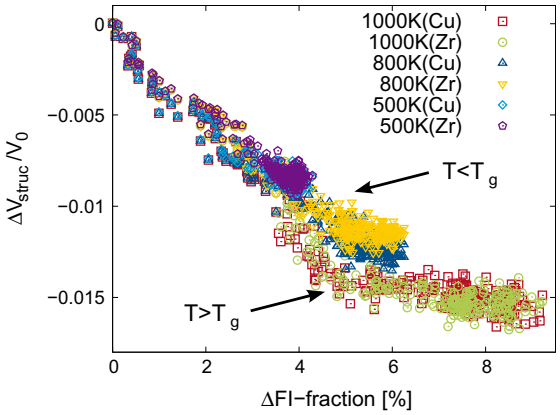

Fig. 5. Correlation between recovery of icosahedral SRO and the release of excess volume.

correlation and we first observe a steeper slope due to faster relaxation of the excess volume, followed by a regime where the Voronoi volumes hardly change despite a further increase in FI fraction. This can again be explained by the packing frustration of icosahedral clusters, as discussed in the previous section for the case of the undeformed sample. In fact, when comparing the final FI fraction after annealing at 1000 K in the SB and undeformed sample (see the marked area in Fig. 4, panel 3c), we find the SB value to be only slightly lower than the final FI fraction in the undeformed sample.

The relaxation mechanisms are thermally activated and, depending on the annealing temperature, different degrees of recovery are achieved during the studied period of time (see also the scans of the final samples after annealing in Fig. 6): After annealing at 500 K, structural inhomogeneities are still present. The average Voronoi volume in the SB is still about 0.7% higher than in the undeformed material, while the volumes in the matrix are about 0.2% lower (see the marked area in panel 1a). At the same time, the FI fraction in the shear band is almost 4% lower than in the matrix (see the marked area in panel 3a). The same trend is found in the CSRO, where considerable differences between the SB and the matrix are still present after annealing (see the marked area in panel 5a). When the deformed sample is annealed at 800 K, which is still below the glass transition temperature, a higher degree of relaxation is obtained since the increased annealing temperature enables the activation of more relaxation mechanisms. Yet we still observe the same amount of excess volume inside the SB (see the marked area in panel 1b), and the TSRO and CSRO in the SB deviate from the matrix (see the marked areas in panels 3b and 5b). If the annealing temperature is above T_g (1000 K), the homogeneous microstructure is recovered and all defects introduced by plastic deformation are fully relaxed (see the marked areas in panels 1c and 3c). At the glass transition, thermal activation is sufficient to activate all mechanisms contributing to structural recovery and, therefore, also structural defects present in the as-prepared glass can be relaxed during

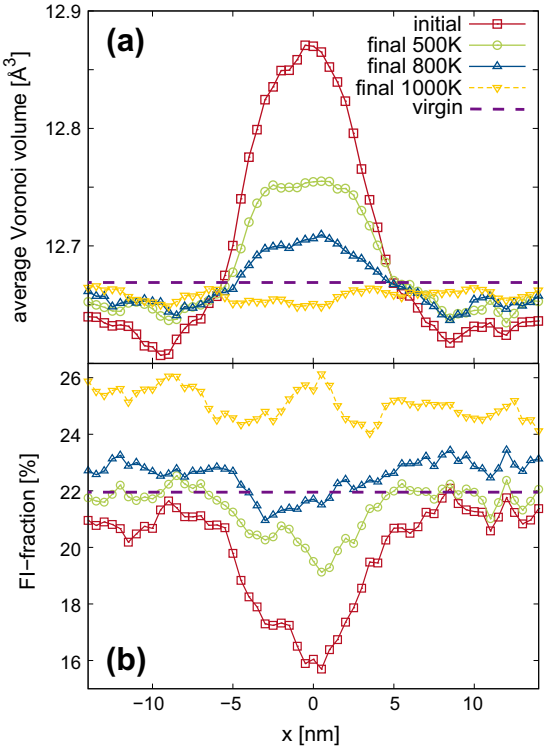

Fig. 6. Linear scans of the deformed sample before (=initial) and after annealing (=final) at 500, 800 and 1000 K, showing (a) the change in average volume of Cu atoms and (b) the recovery of Cu-centered full icosahedra.

annealing, as observed in the case of the undeformed sample (see the previous section). Also, the final FI fraction after annealing (marked area in panel 3c) is about 3% higher than in the as-prepared material (dashed line in panel 3c), both in the SB and the matrix.

Major structural relaxations already occur inside the shear band during heating. The release of excess volume, the FI fraction and the NN correlation indices saturate after a certain annealing time (see rows two, four and five in Fig. 4). This initial ultrafast recovery is not observable with experimental techniques, and will most likely occur during deformation at experimental deformation rates.

In order to extract quantitative information on the relaxation kinetics, we therefore only considered the isothermal part of the volume relaxation. According to Haruyama and Inoue [25], the change in reduced free volume x during isothermal annealing at a temperature below T_g can be fitted by a stretched exponential function

$$x = x_{eq} + (x_0 - x_{eq}) \cdot \exp\left[-\left(\frac{t}{\tau}\right)^{\beta}\right] \quad (8)$$

where x_{eq} is an equilibrium value of the reduced free volume at $t \to \infty$, x_0 is the initial value, τ is the relaxation time and β is the Kohlrausch exponent. We fitted Eq. (8) to the volume relaxation data obtained during annealing of the virgin sample and the shear band in the deformed sample (only for annealing temperatures below T_g). The reduced free volume can be estimated by comparing the density of

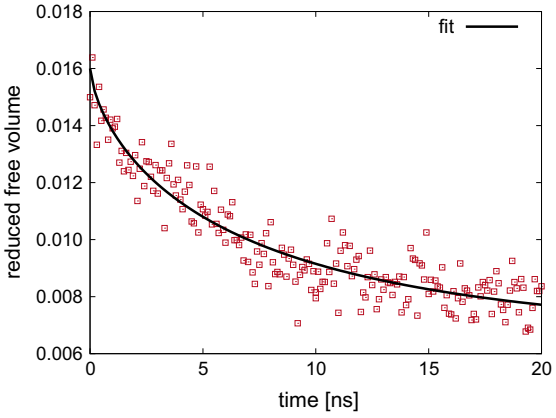

Fig. 7. Isothermal change in free volume during annealing at 800 K. The data was fitted by a stretched exponential function ($\Delta\beta = 4\%$; $\Delta\tau = 3\%$).

the glass to the density of an ideal glass (for details, see Ref. [25]). Due to the lack of data for an ideal glass, we used the value of the undeformed glass after annealing at 1000 K, which we assume to be close enough to the state of a relaxed glass. Since the number density is equal to the reciprocal average Voronoi volume, we calculated the reduced free volume by $x = (\overline{V} - \overline{V}_{ideal})/(0.5 \cdot \overline{V}_{ideal})$, where $\overline{V}$ is the average Voronoi volume in the annealed sample and $\overline{V}_{ideal}$ is the average Voronoi volume in the relaxed glass at the corresponding temperature. Numerical fits to our data (see Fig. 7 as an example) yield a Kohlrausch exponent $\beta = 0.63$, which is in the range of what has been reported in the literature for the isothermal relaxation of metallic glasses below T_g (e.g. Ref. [25]). The Kohlrausch exponent takes values between 0 and 1, where $\beta = 1$ reflects a single activation energy [26], while a smaller value suggests a broad distribution of activation energies. The structural relaxation observed in our simulations is therefore facilitated by a number of processes with different activation barriers. Interestingly, we find the same β for the shear band and the undeformed sample, which indicates that the same processes that occur during the relaxation of an as-prepared metallic glass are involved in the recovery of the highly strained material inside the shear band. The difference, however, is found in the relaxation times, which is 13 times longer in the virgin material as compared to the SB for annealing at 500 K, and 7 times longer for an annealing temperature of 800 K, respectively.

In this section we have studied the structural recovery of a pre-deformed $Cu_{64}Zr_{36}$ glass during thermal annealing at different temperatures below and above T_g. To characterize the relaxation mechanisms, we had to eliminate the effect of thermal expansion from our data by comparing the data for the pre-deformed sample to the data for an undeformed sample. We found that the relaxation of excess volume as well as the recovery of chemical and TSRO contribute to structural recovery. A linear correlation between the increase in packing density with the increase in icosahedral short-range order was found for annealing temperatures below T_g. The recovery mechanisms are thermally

activated and the degree of recovery depends on the annealing temperature: after annealing at 500 and 800 K, structural inhomogeneities were still significant, whereas annealing at a temperature above T_g leads to a homogeneous microstructure with lower excess volume and a higher degree of TSRO as compared to the virgin sample.

3.4. Atomic scale relaxation mechanisms

In order to identify the mechanisms contributing to structural relaxation in shear band and matrix at different temperatures, we utilized the ability of MD simulations to study individual atomic jump processes. Since relaxation mechanisms in the supercooled liquid regime differ from mechanisms in the glassy state and studying individual jumps becomes more difficult due to high atomic mobilities, we limited the characterization of relaxation mechanisms to temperatures below T_g. During a time interval of 20 ns at constant temperature, the jump lengths inside SB and matrix were evaluated for both atomic species and the resulting distributions were plotted in Fig. 8. Again, we performed the same analysis for the undeformed sample for comparison. At an annealing temperature of 500 K the jump length distributions for the undeformed sample, as well as for the SB and matrix in the predeformed sample contain only one peak. This peak originates from displacements much shorter than the NN distance (≈2.6 Å for Cu–Cu neighbors) and is therefore referred to as original site peak (OSP). This observation is typical for metallic glasses and hints to a collective diffusion mechanism where groups of atoms jump in concert. Due to the lacking particular length scale for displacements in the glassy state, atomic jumps lead to a Gaussian-like broadening of the OSP with time, while different atomic mobilities, i.e., dynamic heterogeneities, are reflected in a deviation from Gaussianity and tails to longer distances [27,28]. The OSP for the matrix of the deformed sample is broadened as compared to the virgin sample and shifted to larger displacements, which indicates a higher mean square displacement and thus higher diffusivity. In the case of the shear band, the peak is located at even higher displacements and the peak broadening is significantly stronger as compared to the matrix, with a pronounced tail to larger jump lengths. This is in good agreement with the above findings of an increased excess volume in the heavily deformed material in the shear band. Interestingly, the distributions for Cu and Zr atoms are almost identical for shear band and matrix, as well as for the virgin material, despite the significant size difference, and therefore supposedly increased mobility of Cu atoms. This is a typical feature of a collective jump process that is hardly influenced by individual atomic mobilities [27].

We next characterized collective jumps in the SB and matrix qualitatively as well as quantitatively, to confirm the assumption of collective motion as the dominant relaxation mechanism at 500 K. For detecting individual jump events we ignore atoms with a displacement below 1 Å; the remaining atoms are divided into clusters by

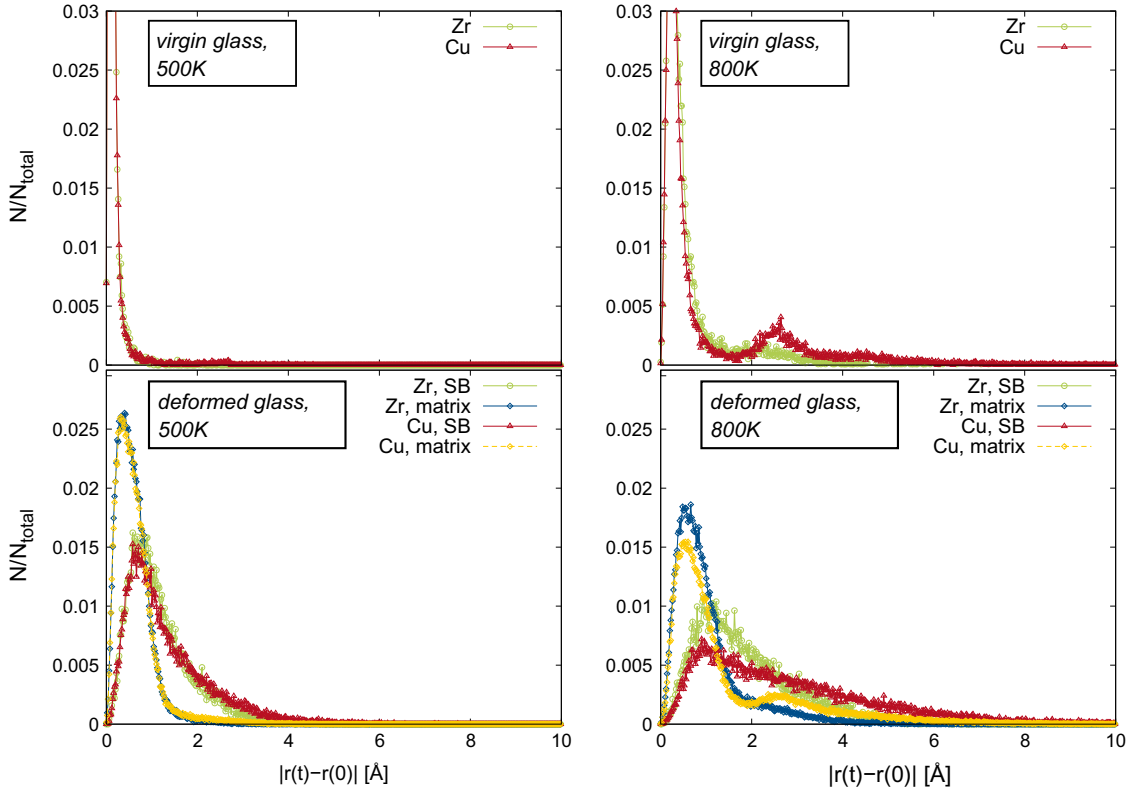

Fig. 8. Jump length distribution for undeformed and deformed samples after $\Delta t = 20$ ns during annealing at different temperatures.

analyzing the nearest neighbor environment: if two atoms are nearest neighbors and have both jumped within a time interval of 200 ps, they are assumed to belong to the same jump event. For a quantitative analysis of the collective jump process, we plotted the probability distribution $P(n)$ of the chain length n for different test volumes in the deformed and undeformed sample at the beginning of isothermal annealing and after 20 ns (Fig. 9); for better statistics, we averaged over three individual distributions. At the beginning of annealing at 500 K, collective jumps inside the SB involve up to 106 atoms and the average chain length is considerably higher than in the matrix (Fig. 9b), where the maximum chain length is only 42 atoms. After 20 ns at 500 K (Fig. 9c), the maximum chain length in both the SB and the matrix is decreased to 15 atoms, which is close to the value we observe for the virgin sample (Fig. 9a). This is in good agreement with the spatial distribution of atomic jumps given in Fig. 10, where at the beginning of annealing (=start) we observe a considerably higher frequency of atomic jumps in the SB as compared to the matrix, while after 20 ns at 500 K the distribution of diffusive jumps is homogeneously distributed in the whole sample and the overall frequency of jumps is smaller than at the beginning of annealing. When analyzing individual collective jumps at the beginning of annealing, as displayed in Fig. 11, we find that at 500 K most atoms jump in a chain-type process in the matrix as well as in the SB. While the chains in the matrix are mostly linear, the collective jumps in the SB are mostly longer, more complex chains containing several branches.

During annealing at 800 K, an additional process contributes to structural relaxation: the jump length distributions for Cu atoms (see Fig. 8c and d) contain an additional feature besides the OSP at about 2.6 Å, which is equal to the Cu–Cu nearest neighbor distance. In the case of the virgin sample and the matrix of the deformed sample, the additional peak is clearly resolvable; in the SB, however, the OSP broadening is so strong that the NN peak is only visible as a hump in the distribution. Due to the elevated temperature, Cu atoms are able to perform nearest neighbor jumps in addition to their contribution to collective motion. The bigger Zr atoms are less mobile and the frequency of Zr nearest neighbor jumps is not significant; therefore, no additional peak appears in the Zr distribution. The broad distribution of jump lengths in the SB with a long-range tail of up to several NN distances can be explained by secondary jumps during the studied time interval of 20 ns. Comparing the chain length distributions for 500 K (Fig. 9a–c) and 800 K (Fig. 9d–f), we find a higher number of atoms per collective jump at an annealing temperature of 800 K in both the SB and the matrix, as well as in the undeformed sample. This is in good agreement with what is known about collective motion in metallic glasses, where an increase in temperature results in longer chains and larger individual displacements [29]. Again, the number of atoms involved in one individual jump process is considerably higher at the beginning of isothermal annealing (Fig. 9e) than after 20 ns (Fig. 9f). The nature of individual collective jumps at the beginning of annealing at 800 K (see Fig. 11) is also chain-like. In the matrix, the atomic chains are still mostly linear, but branched chains are found more frequently than at 500 K. Apart from a number of chains with less than 10 atoms, which are mostly linear, collective jumps in the SB at 800 K are complex

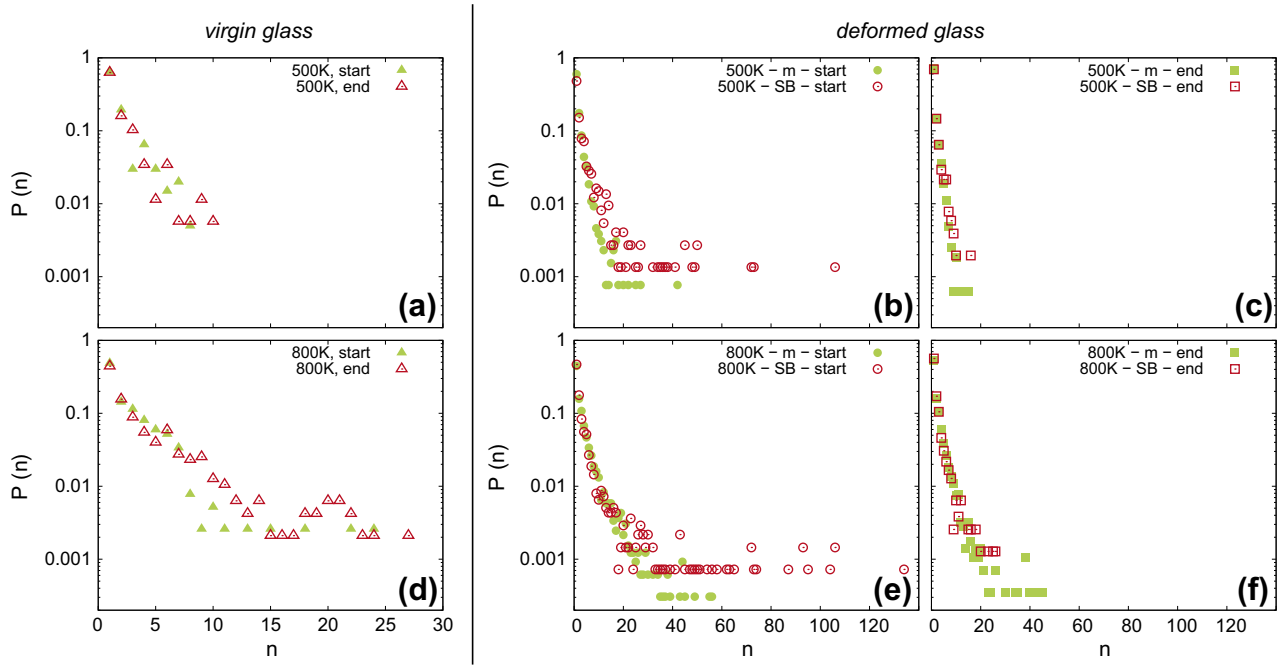

Fig. 9. Probability distribution $P(n)$ of chain length n (=number of atoms involved in a collective jump event) during annealing at 500 K (a–c) and 800 K (d–f) for undeformed and deformed $Cu_{64}Zr_{36}$ glass. For the deformed samples we analyzed $P(n)$ at the beginning of isothermal annealing (=start) and after 20 ns (=end); the evaluated time interval was 200 ps in all cases.

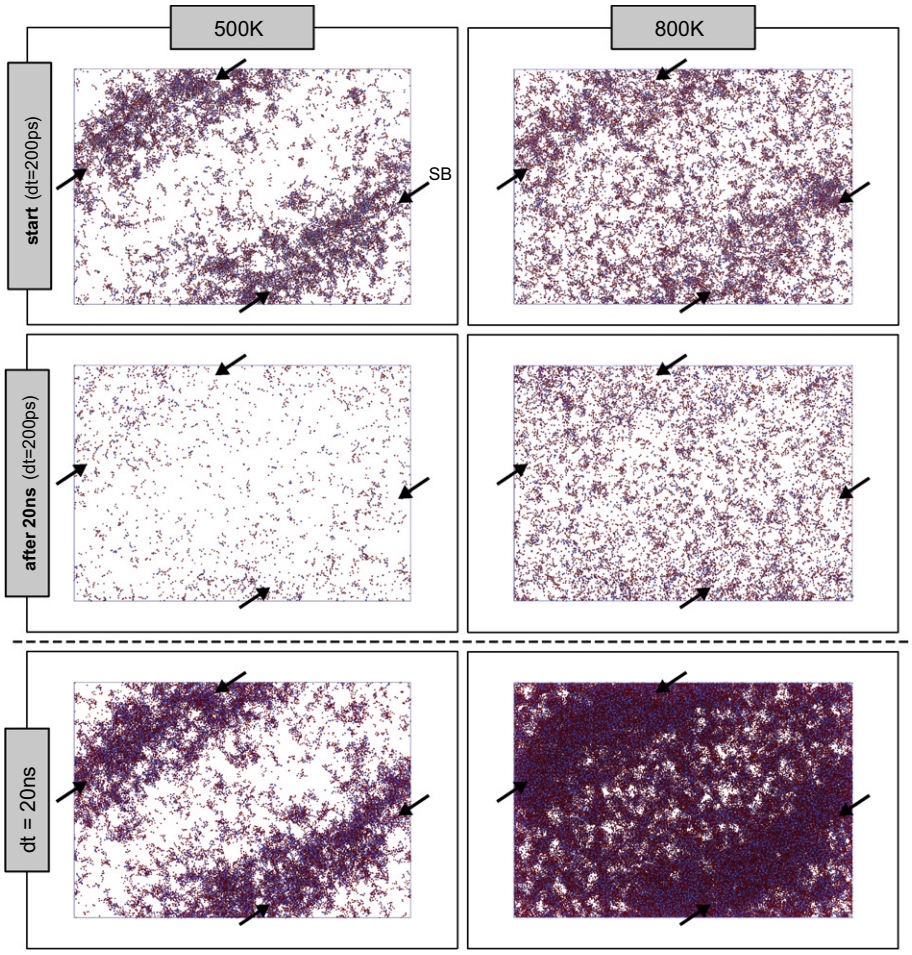

Fig. 10. Atomic displacements in the whole sample during recovery annealing at 500 K and 800 K at the beginning of isothermal annealing (=start, top row), after 20 ns annealing (middle row) and for the total annealing time of 20 ns (bottom row). The arrows mark the position of the shear band. Only atoms with atomic displacements larger than 1.0 Å for annealing at 500 K and 1.2 Å for annealing at 800 K are displayed; red atoms are Cu, blue atoms Zr. (For interpretation of the references to color in this figure legend, the reader is referred to the web version of this article.)

networks of branched chains involving a large number of atoms. These clusters of jumping atoms are evocative of a flow-like motion, as typically found in the undercooled melt (e.g. [30]). The spatial distribution of diffusional jumps in the deformed sample (see Fig. 10 (right)) shows that at 800 K structural rearrangements occur in the whole sample and are not limited to the SB, as observed during annealing at 500 K. This is in line with the findings above, where we hardly observed structural relaxations in the matrix at 500 K in contrast to a significant recovery of short-range order at 800 K. Another characteristic of the relaxation mechanism becomes obvious when taking a closer look at the distribution of atomic displacements during the total annealing time of 20 ns (see Fig. 10 (bottom)): the diffusive jumps are not homogeneously distributed, but the images suggest that mobile atoms have jumped in chains between a network of immobile atoms. This interpretation would fit to the observed non-Gaussian nature in the jump length distribution (Fig. 8), which, as mentioned before, is related to the dynamic heterogeneity of the relaxation mechanism.

The characterization of individual atomic jumps has shed light on the atomistic mechanisms carrying structural relaxations in pre-deformed metallic glass: at an annealing temperature of 500 K, structural relaxations occur solely by collective jumps in a chain-type process, while at 800 K, two processes contribute to structural relaxation, namely nearest neighbor jumps of the small Cu atoms and collective motion. The individual atomic displacements as well as the number of atoms involved in one collective jump were higher at 800 K as compared to 500 K, and the chains often contained branches at the elevated annealing temperature. At the beginning of isothermal annealing we found enhanced atomic rearrangements in the shear band at both temperatures, which occured by cooperative jumps of a large number of atoms in complex clusters instead of linear chains, similar to flow-like motion in supercooled liquids. After 20 ns of relaxation, atomic rearrangements occurred in the whole sample with the same frequency, and the chain length distributions were similar in the SB and matrix.

These results are also relevant for understanding the precipitation of crystalline phases in shear bands. Experimental studies revealed that, during deformation at low homologous temperatures, nanocrystallites preferentially

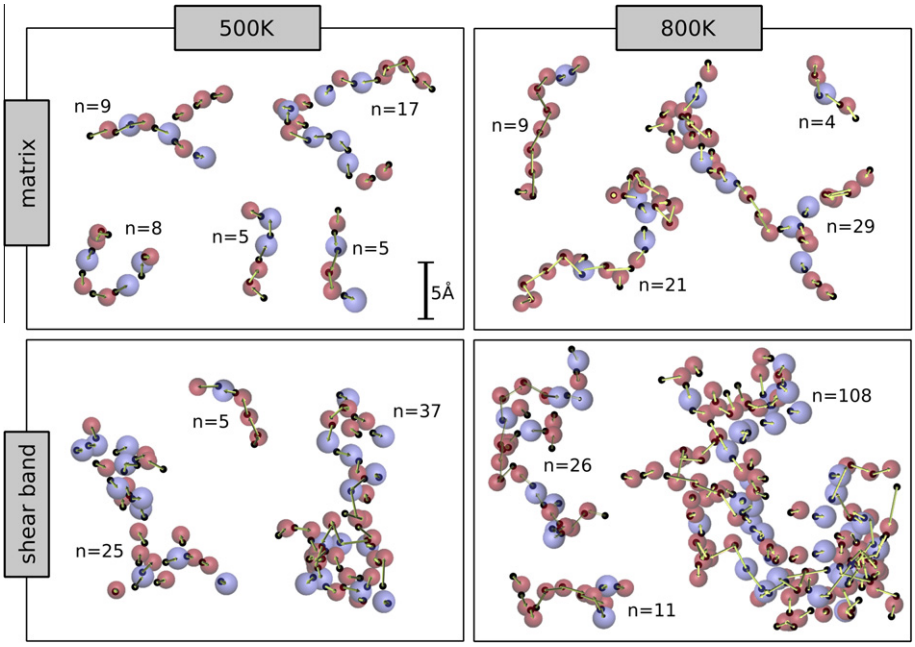

Fig. 11. Collective jumps in shear band and matrix at the beginning of annealing at 500 and 800 K during a time interval of 200 ps. Red and blue spheres represent Cu and Zr atoms at $t = 200$ ps, while the black dots represent the initial positions at $t = 0$; the arrows represent the atomic displacement vectors. (For interpretation of the references to color in this figure legend, the reader is referred to the web version of this article.)

form inside shear bands [31,32]. This observation was explained by increased atomic mobilities in SBs as a consequence of flow dilatation, which was supported by experiments on glassy polymers where increased mobilities inside SBs were measured directly [33]. At first glance, this appears contradictory to the current study, where enhanced atomic mobilities inside SBs were only detected within the first few nanoseconds of thermal annealing, timescales not sufficient for crystal formation. However, if crystallization or diffusion is studied in situ during deformation, where the generation and annihilation of excess volume occur simultaneously, we expect increased diffusivities along SBs as long as a sample is strained. For the case of a pre-deformed sample subjected to thermal annealing, on the other hand, our results predict no enhanced diffusivity in the SBs. Instead, we assume that enhanced nucleation kinetics are a result of decreased nucleation barriers for crystalline phases in an SB due to defects in the short and medium range orders.

4. Conclusions

In conclusion, we have studied structural changes in a $Cu_{64}Zr_{36}$ glass during plastic deformation and thermal annealing at different temperatures above and below T_g. We found that a shear band in this metallic glass is characterized by an increased excess volume, a lower degree of TSRO and a modified CSRO. The TSRO and CSRO in the surrounding matrix are hardly affected, but the density is increased due to a compressive strain introduced by the SB. Considering these results, it is not surprising that structural recovery during thermal annealing involves the relaxation of excess volume, topological and CSRO. The release of excess volume and the recovery of icosahedral short-range order are linearly coupled for temperatures below T_g. If a critical FI fraction is reached, however, the excess volume remains constant due to packing frustration. Depending on the temperature, different degrees of recovery were achieved during 20 ns of isothermal annealing: a full recovery of the SB was only observed for an annealing temperature above T_g, while after annealing at 500 and 800 K substantial structural inhomogeneities remained. A detailed analysis of the atomistic mechanisms contributing to structural relaxation revealed that at 500 K collective motion is the only relevant relaxation mechanism, unlike at 800 K, where Cu nearest neighbor jumps occur in addition to cooperative atomic jumps. The number of atoms per jump and the individual atomic displacements are higher at 800 K than at 500 K. The collective jumps showed characteristics of a chain-type process with mostly linear chains. At the beginning of isothermal annealing, however, we found jumps involving a large number of atoms in complex clusters or highly branched chains in the SB, similar to flow-like motion in supercooled liquids. Moreover, we found a larger thermal expansion for Cu atoms as compared to Zr atoms, caused by the stronger anharmonicity in the interatomic potential for Cu.

Going back to our introductory remark on the discrepancy between free volume theory and experimental observations: our results provide a link between free volume theory, which predicts instantaneous recovery of shear bands at elevated temperatures due to locally increased atomic mobilities like in the supercooled liquid, and experiments, where shear bands recover on timescales in the

range of hours. At the beginning of annealing, we observe relaxation mechanisms in the shear band as typically found in the supercooled liquid state. Yet, due to the fast annihilation of excess volume in this regime, the atomic mobilities in the shear band decrease rapidly and after 20 ns annealing no enhanced diffusivity is found in the shear band anymore. A full recovery on short timescales is therefore inhibited.

Acknowledgements

The authors acknowledge financial support by the Deutsche Forschungsgemeinschaft (DFG) through Project Grant No. Al-578/13-1. A DAAD-PPP travel grant is also acknowledged. Computing time was made available by HHLR Frankfurt and Darmstadt, as well as by CSC Julich.

References

[1] Pampillo CA. Scripta Metall 1972;6:915.
[2] Wright WJ, Hufnagel TC, Nix WD. J Appl Phys 2003;93:1432.
[3] Hajlaoui K, Benameur T, Vaughan G, Yavari AR. Scripta Mater 2004;51:843.
[4] Li QK, Li M. Appl Phys Lett 2006;88:241903.
[5] Jiang WH, Pinkerton FE, Atzmon M. Acta Mater 2005;53:3469.
[6] Cao QP et al. Acta Mater 2010;58:1276.
[7] Lee MH et al. Scripta Mater 2010;62:678.
[8] Xie S, George EP. Acta Mater 2008;56:5202.
[9] Krishnanand KD, Cahn RW. Scripta Metall 1975;9:1259.
[10] Xu YL, Hahn H, Li JG. Intermetallics 2010;18:2039.
[11] Nagel C, Ratzke K, Schmidtke E, Faupel F. Phys Rev B 1999;60:9212.
[12] Taub AI, Spaepen F. Acta Metall 1980;28:1781.
[13] Plimpton S. J Comput Phys 1995;117:1.
[14] Mendelev MI, Sordelet DJ, Kramer MJ. J Appl Phys 2007;102:043501.
[15] Cheng YQ, Cao AJ, Sheng HW, Ma E. Acta Mater 2008;56:5263.
[16] Voronoi GZ. J Reine Angew Math 1908;134:199.
[17] Brostow W, Chybicki M, Laskowski R, Rybicki J. Phys Rev B 1998;57:13448.
[18] Lee JC et al. J Mater Res 2007;22:3087.
[19] Cheng YQ, Cao AJ, Ma E. Acta Mater 2009;57:3253.
[20] Turnbull D, Cohen MH. J Chem Phys 1961;34:120.
[21] Li M et al. Phys Rev B 2009;80:184201.
[22] Shimizu F, Ogata S, Li J. Mater Trans 2007;48:2923.
[23] Birch F. J Geophys Res 1952;57:227.
[24] Wallace DC. Thermodynamics of crystals. New York: John Wiley & Sons; 1972.
[25] Haruyama O, Inoue A. Appl Phys Lett 2006;88:131906.
[26] Jackle J. Rep Prog Phys 1986;49:171.
[27] Donati C et al. Phys Rev Lett 1998;80:2338.
[28] Caprion D, Matsui J, Schober HR. Phys Rev Lett 2000;85:4293.
[29] Faupel F et al. Rev Mod Phys 2003;75:237.
[30] Gaukel C, Schober HR. Solid State Commun 1998;107:1.
[31] Kim JJ, Choi Y, Suresh S, Argon AS. Science 2002;295:654.
[32] Wilde G, Rosner H. Appl Phys Lett 2011;98:251904.
[33] Zhou QY, Argon AS, Cohen RE. Polymer 2001;42:613.